



Revisiting the relationship between soil moisture and N₂O production pathways by measuring ¹⁵N₂O isotopomers

Kate A. Congreves¹, Trang Phan¹, and Richard E. Farrell²

¹Department of Plant Sciences, ²Department of Soil Science, University of Saskatchewan, Saskatoon, SK S7N 5A8

5 Correspondence to: Kate A. Congreves (kate.congreves@usask.ca)

Abstract

Understanding the production pathways of potent greenhouse gases, such as nitrous oxide (N₂O), is essential for accurate flux prediction and for developing effective adaptation and mitigation strategies in response to climate change. Yet, there remain surprising gaps in our understanding and precise quantification of the underlying production pathways – such as the relationship between soil moisture and N₂O production pathways. A powerful, but arguably underutilized, approach for quantifying the relative contribution of nitrification and denitrification to N₂O production involves determining ¹⁵N₂O isotopomers and ¹⁵N site preference (SP) via spectroscopic techniques. Using one such technique we conducted a short-term incubation to precisely quantify the relationship between soil moisture and N₂O production pathways. For each of three soils, microcosms were arranged in a complete random design with four replicates; each microcosm consisted of air-dried soil packed into plastic petri dishes wherein moisture treatments were established for water contents equivalent to 45 to 105% water-filled pore space (WFPS). The microcosms were placed in 1-L jars and sealed; headspace samples were collected after 24-h and analyzed for total N₂O concentrations using gas chromatography, and for ¹⁵N₂O isotopomers using cavity ring-down spectroscopy. Relatively low N₂O fluxes and high SP values indicated nitrification during dry soil conditions, whereas at higher soil moisture, peak N₂O emissions coincided with a sharp decline in SP indicating denitrification. This pattern supports the classic N₂O production curves from nitrification and denitrification as inferred by earlier research; however, our isotopomer data enabled the quantification of source partitioning for either pathway thereby providing clarity on N₂O sources during the transition from nitrification to denitrification. At soil moisture levels < 53% WFPS, the fraction of N₂O emitted was predominately attributed to nitrification but thereafter decreased rapidly, according to: $F_N = 3.19 - 0.041x$, until a WFPS of 78%. Simultaneously, from WFPS of 53 to 78%, the fraction of N₂O that was attributed to denitrification was modelled as: $F_D = -2.19 + 0.041x$; at moisture levels of > 78%, denitrification completely dominated. Clearly, the soil moisture levels during transition is a key regulation of N₂O production pathways.

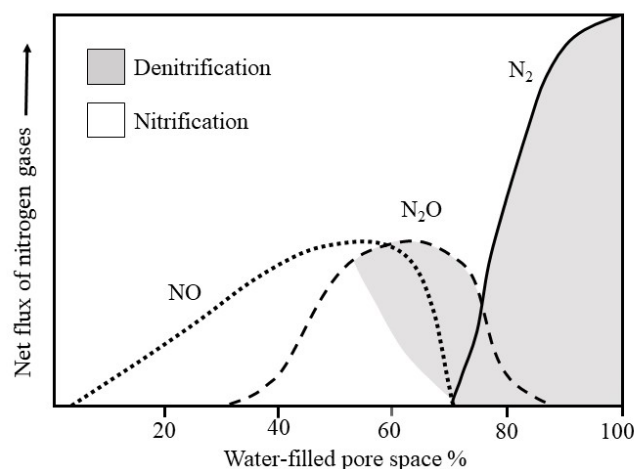
1. Introduction

30 Soils are the largest source of anthropogenic N₂O emissions, representing up to 80% of total N₂O emissions (Environment Canada., 2015). Understanding the mechanisms leading to the emission of this potent greenhouse gas is essential for accurate flux prediction and for developing effective adaptation and mitigation strategies in response to climate change. Decades of research have strengthened our understanding of N₂O fluxes—namely, how N₂O



production is regulated by soil oxygen, substrate availability, and microbial activity (Butterbach-Bahl et al., 2013; Chapuis-Lardy et al., 2007; Wagner-Riddle et al., 2017); how N₂O emission is regulated by advection, solubility and diffusion (Balaine et al., 2013; Clough et al., 2005). However, there remain surprising gaps in our understanding of the underlying mechanisms, one such area being the relationship between soil moisture and N₂O production pathways.

- 5 Nitrous oxide is a product of nitrification and denitrification—microbially driven processes that depend on the aeration status of the soil (Banerjee et al., 2016; Barnard et al., 2005). As a result, the relative contributions of nitrification and denitrification are often determined based on their relationship to soil water-filled-pore space (WFPS), which acts as a proxy for aeration status. However, the widely cited relationship between soil N₂O production and soil moisture (Fig. 1) is actually an educated deduction that blends work from two different studies, from which the N₂O production pathways are inferred (Davidson, 1991; Linn and Doran, 1984). As such, it may be argued that the precise relationship between soil water content and N₂O production mechanisms remains unknown and requires more complete quantification. Developing a more precise relationship is necessary for improving our capacity to understand and predict N₂O production mechanisms.
- 10



- 15 **Figure 1 Relative contributions of nitrification and denitrification processes to N₂O production as a function of water-filled pore space (adapted from Davidson 1991).**

- Isotopomers (i.e., isomers having the same number of each isotopic atom, but differing in their position) provide a powerful and novel approach for quantifying the relative contribution of N₂O producing processes via nitrification and denitrification (Van Groenigen et al., 2015). The isotopomers of N₂O (i.e., ¹⁴N¹⁵NO and ¹⁵N¹⁴NO) can be quantified using advanced laser spectroscopic approaches—including cavity ring-down spectroscopy (CRDS)—that enable the intramolecular ¹⁵N distribution of N₂O to be determined (Mohn et al., 2014). The difference between the abundance of ¹⁵N within the central (alpha, α) and the terminal (beta, β) N atoms of the linear N₂O molecule is expressed as site-preference (SP), and high SP values of 13 to 37‰ are attributed to nitrification (hydroxylamine oxidation) while SP values of 0‰ or less indicate nitrite or nitrate reduction (denitrification and nitrifier
- 20



denitrification) (Denk et al., 2017; Ostrom et al., 2010; Sutka et al., 2006; Toyoda et al., 2005). The underlying reason for the distinct differences in SP values of N₂O from either microbial pathway is due to primary kinetic isotope effects when N₂O is produced (Popp et al., 2002).

Our objectives were to precisely quantify the relationship between soil moisture and N₂O production by measuring ¹⁵N₂O isotopomers; and evaluate the variability in this relationship based on differences in soil nutrient levels, organic matter, and texture. The term “isotopomer” is used herein to indicate molecules of the same mass in which the trace isotopes are arranged differently. This differs from “isotopologue”, which is a more general term referring to molecules that differ in isotopic composition.

2. Materials and Methods

2.1 Soil collection and characterization

Surface (0–10 cm) soils representing different nutrient levels and texture classes were collected from three locations in the Dark Brown soil zone in Saskatchewan, Canada. The soils—classified as Dark Brown Chernozems of the Sutherland, Asquith and Bradwell associations—were collected using a shovel, air dried and sub-samples were shipped to A&L Laboratories Inc (London, ON) for analysis (Table 1). For additional characterization, sub-samples were analyzed at the University of Saskatchewan for equilibrium soil water content, soil inorganic N levels, soil total N concentration and ¹⁵N abundance (Table 1). The equilibrium soil water was determined via the long-column method based on the average of four technical replicates (Reynolds and Topp, 2007). Initial soil NO₃⁻ and NH₄⁺ concentrations were determined in quadruplicate using the KCl extraction method of Maynard et al. (2007); briefly, 5 g soil was mixed with 50 mL of 2 M KCl, shaken for 30-min, filtered through Whatman 42 filter paper, and the extracts frozen at -20°C until they could be analyzed. For analysis, the extracts were thawed and allowed to equilibrate to room temperature before being analyzed using air segmented (continuous) flow analysis with a SEAL AA3 HR chemistry analyzer (SEAL Analytical; Kitchener, ON). Soil total N concentration (%) and ¹⁵N content (atom%) were determined in duplicate using a Costech ECS4010 elemental analyzer (Costech Analytical Technologies Inc., Valencia CA) coupled to a high-precision Delta V mass spectrometer (Bremen, Germany) with a precision of 0.06‰ for δ¹⁵N. Chickpea flour with an atom% ¹⁵N = 0.3691 was used as a lab reference.

2.2 Incubation experimental design

For the incubation study, soil microcosms were arranged in a randomized complete design with four replicates. For each microcosm, air-dried soil was packed into a small (5.9 cm i.d. × 0.80 cm tall) plastic petri dish. The mass of soil needed to fill the petri dish varied with texture—ranging from 22.0 g to 29.0 g—and yielded soil bulk densities of 1.01, 1.10, and 1.33 g cm⁻³ for the Sutherland, Asquith, and Bradwell soils, respectively. While the quantities and bulk densities differed for each soil type, it was essential that the soil completely fill the petri dishes to avoid any differences in soil surface boundary layer or gas diffusion that would alter N₂O emission.



Soil moisture treatments were based on gravimetric soil water content (θ_g) established by adding deionized water to the soil microcosms, using a fine mist of water applied from a manual spray bottle, to a predetermined weight. Gravimetric soil moisture content was varied to yield a water-filled pore space (WFPS) between 45 and 105%.

The gravimetric water, volumetric water, and WFPS were determined according to Eq. (1-3):

5

$$\text{Gravimetric water } \theta_g (\text{g H}_2\text{O g soil}^{-1}) = \frac{\text{water added (g)}}{\text{dry soil (g)}} \quad (1)$$

$$\text{Volumetric water } \theta_v (\text{cm}^3 \text{H}_2\text{O cm}^3 \text{soil}^{-1}) = \theta_g \times BD \quad (2)$$

10

$$\% \text{ WFPS} = \left[\frac{\theta_v}{\left(1 - \frac{BD}{PD}\right)} \right] \times 100 \quad (3)$$

where, BD denotes soil bulk density and PD denotes particle density (PD), which was assumed to be 2.65 g cm⁻³.

15 Immediately after moistening the soil microcosm, the petri dish was sealed inside a 1L wide-mouth mason jar fitted with a gas sampling septum, and time of sealing was recorded. Blank jars containing an empty petri dish were set up to account for background (atmospheric) gas concentrations. The microcosms were incubated at 22°C ± 1°C.

2.3 Sampling and analysis

20 After 24-hrs, a headspace gas sample was collected from each microcosm (with the time of sampling recorded) using a 20-mL plastic syringe fitted with a 22-gauge needle, injected into an evacuated 12-mL Exetainer[®] tube (Labco Limited, UK), and analyzed for N₂O, CO₂, and O₂ concentration using gas chromatography (Bruker 450 GC, Bruker Biosciences, Billerica, MA). A separate 30-mL gas sample was collected from each microcosm, injected into an evacuated 12-mL Exetainer[®] tube, and analyzed for ¹⁵N₂O concentration, $\delta^{15}\text{N}_\alpha$, $\delta^{15}\text{N}_\beta$, and $\delta^{18}\text{O}$ using a CRDS-based Picarro G5131-*i* isotopic N₂O analyzer (Picarro Inc.; Santa Clara, CA).

2.4 Isotopomer approach using ¹⁵N site preference and $\delta^{18}\text{O}$ for N₂O source identification

25 Site preference was calculated by subtracting the abundance of ¹⁵N from the terminal N atom (beta, β) from that of the central (alpha, α) N atom. The fraction of N₂O derived from hydroxylamine oxidation during nitrification (F_N) or the reduction of nitrate or nitrite during denitrification (F_D) was estimated by adopting the isotopomer mixing approach described by Deppe et al. (2017) and using the SP and $\delta^{18}\text{O}$ values of gas samples collected from the different soils. As suggested by Well et al. (2012), and because SP was more closely correlated to $\delta^{18}\text{O}$ ($r = 0.906$) than $\delta^{15}\text{N}$ ($r =$
30 0.849), we used $\delta^{18}\text{O}$ instead of $\delta^{15}\text{N}$. Equations (4) and (5) show the source partitioning calculations.



$$F_N = \frac{SP - SP_D}{SP_N - SP_D} \quad (4)$$

$$F_D = 1 - F_N \quad (5)$$

5 where F_N and F_D indicate the fraction of N_2O derived from nitrification or denitrification, respectively, using SP endmembers for nitrification (SP_N) and denitrification (SP_D).

Endmembers for SP_D to SP_N were set at: 2.0 to 23.7; 0.7 to 21.7; 14.4 to 23.3 for the Sutherland, Asquith, and Bradwell soils, respectively. Endmembers for $\delta^{18}O_D$ to $\delta^{18}O_N$ were set at: 16.0 to 35.1; 18.8 to 39.5; 25.4 to 34.2 for the Sutherland, Asquith, and Bradwell soils, respectively. The endmember ranges were based on our data where
 10 $SP_N/\delta^{18}O_N$ represented the average values before the transition zone from nitrification to denitrification-dominated N_2O production; $SP_D/\delta^{18}O_D$ represented the lowest values during denitrification for each soil type.

For source partitioning, the influence of N_2O reduction to N_2 on SP was taken into account by using the reduction and mixing line intercept approach – as described by Deppe et al., (2017). However, rather than using an estimated reduction line derived from the literature, we calculated the slope and intercept for the reduction line based on our
 15 data: the $SP/\delta^{18}O$ plot for the soil moisture range after the transition zone for each soil type. The point of intersection between the endmember mixing line and the reduction line gave the estimated initial isotope values (SP^* , ^{18}O) of produced N_2O before reduction to N_2 . In the soil moisture range after the transition from nitrification to denitrification, if the SP^* value was higher than the measured SP value of the gas sample, the measured SP value was used since N_2O reduction was assumed to be negligible. The F_N and F_D were then calculated from SP values (or SP^*) and the SP
 20 values of the nitrification and denitrification endmembers. This calculation was done for each soil type separately.

2.5 Statistical analysis

Correlation and linear regression analyses were conducted in CoStat (CoStat 6.451, CoHort.com) to determine associations between soil moisture and SP.

3. Results and Discussion

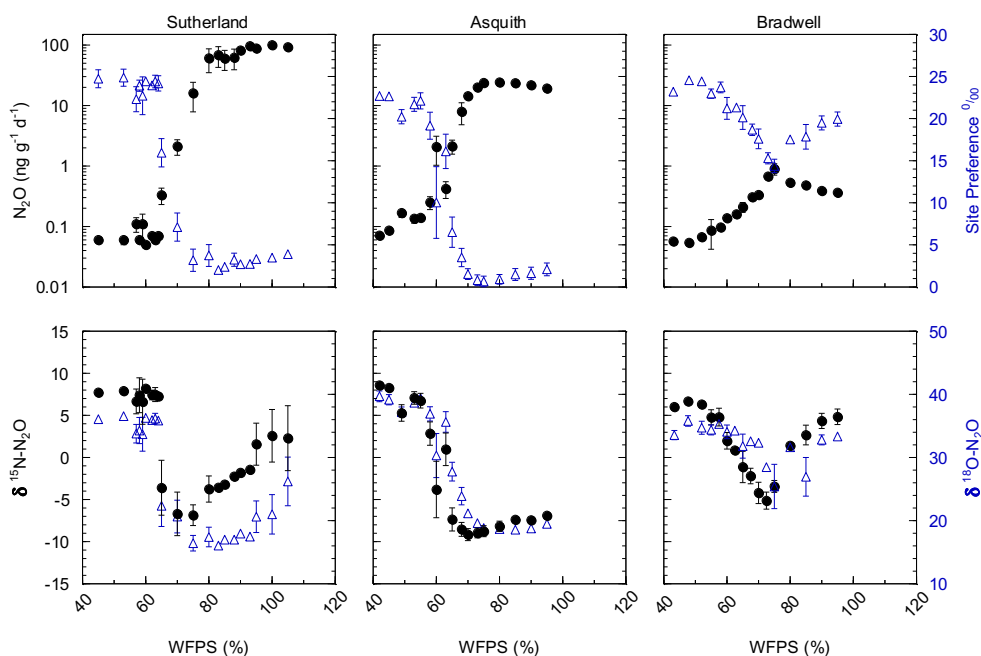
25 3.1 Nitrous oxide fluxes

The three soil types resulted in dramatically different magnitudes of N_2O fluxes. Maximum N_2O fluxes were 100-fold greater from the Sutherland soil ($100 \text{ ng } N_2O\text{-N } g^{-1} \text{ d}^{-1}$) compared to the Bradwell soil ($1 \text{ ng } N_2O\text{-N } g^{-1} \text{ d}^{-1}$), whereas the Asquith soil had more moderate N_2O emissions up to $24 \text{ ng } N_2O\text{-N } g^{-1} \text{ d}^{-1}$ (Fig. 2). The differentiation follows the same trend as soil inorganic N availability and soil organic matter, which decreased in the order: Sutherland > Asquith
 30 > Bradwell (Table 1).

Regardless of the amount of N_2O emitted, there were similarities in how soil moisture levels influenced the relative amount of N_2O produced. For all soil types, relatively low N_2O fluxes were associated with drier soil treatments; N_2O



fluxes were incrementally magnified as soil moisture levels increased from about 55 to 80% WFPS (Fig. 2, top panels). Fluxes either remained relatively high as moisture levels exceeded ~ 80% WFPS, as was the case for the Sutherland soil, or decreased slightly, as observed for the Asquith and Bradwell soils.



5 **Figure 2** Top panels: N_2O emissions as influenced by soil water filled pore space (WFPS), (black ink, left axis); corresponding $^{15}N_2O$ isotopomer site preference (SP), (blue ink, right axis). Bottom panels: $\delta^{15}N$ (black ink, left axis) and $\delta^{18}O$ (blue ink, right axis) of emitted N_2O as influenced by soil water filled pore space (WFPS). Note: N_2O emissions were plotted on a \log_{10} scale to accommodate the large range in emissions from the different soils.

3.2 Nitrous oxide ^{15}N site preference, $\delta^{15}N$ and $\delta^{18}O$

10 Not only total N_2O concentration, but the ^{15}N SP, $\delta^{15}N$ and $\delta^{18}O$ of N_2O changed with soil moisture level, and in parallel with each other (Fig. 2, bottom panels). We identified three moisture ranges—differing slightly for each soil (Table 2)—that regulated N_2O production pathways based on distinct SP, $\delta^{15}N$ and $\delta^{18}O$ values (Fig. 2).

For each soil, the $\delta^{15}N$ and $\delta^{18}O$ values decreased in the same soil moisture region in which the SP values decreased (Fig. 2, bottom panels). Based on the patterns for N_2O fluxes, SP, $\delta^{15}N$ and $\delta^{18}O$ values as related to soil moisture
 15 (Fig. 2; Table 2), our results visually indicate there was a transition between nitrification-derived and denitrification-derived N_2O production at between 64 and 83; 58 and 75; 63 and 75% WFPS for the Sutherland, Asquith, and Bradwell soils, respectively.



Prior to the transition in N₂O production pathway, when the soil was relatively dry, the SP values averaged 23.7, 23.3, and 21.7‰ from the Sutherland, Asquith, and Bradwell soils, respectively. These values are in line with expected SP values attributed to nitrification (Denk et al., 2017; Ostrom et al., 2010; Sutka et al., 2006; Toyoda et al., 2005). Furthermore, the observed consistency among soil types – and the negligible (near 0) slopes between WFPS and ¹⁵N SP – suggests that average SPs during nitrification are relatively insensitive to the rate of production or associated N₂O accumulation. It is known that isotopic fractionation governed by kinetic isotope effects occurs during the reaction sequence NH₄⁺ → NH₂OH → NOH → NO → N₂O and NH₄⁺ → NO₂ → NO → N₂O; however, oxidation of NOH does not involve a primary kinetic isotope effect and thus should not markedly affect SP (Popp et al., 2002).

During the transition from nitrification to denitrification, SP rapidly declined in all soils (Fig. 2, Table 2). The lowest SP values were 2.0, 0.7, and 14.4‰ for the Sutherland, Asquith, and Bradwell soils, respectively. In general, sharp slopes characterized the decline in SP values with increasing soil moisture during the transition; but the Sutherland and Asquith soils had steeper slopes than the Bradwell soil (Table 2). This difference was likely related to differences in soil inorganic or mineralizable N availability (Table 1) and possibly also to differences in the rates of denitrification.

After the transition to denitrification, the SP values increased slightly as soil moisture increased (Table 2) – but more so for the Bradwell soil than the Sutherland and Asquith soils. This finding supports the sensitivity of SP values to the degree of stepwise completion of denitrification (N₂O reduction to N₂). We hypothesize that the ratio of N₂O produced to N₂O reduced was lowest from the Bradwell soil. Contrary to the large accrual of N₂O from the Sutherland and Asquith soils, the low concentration of N₂O produced from the Bradwell soil likely favoured complete reduction (i.e., tighter ‘holes-in-the-pipe’) – causing the Bradwell soil SP values to be the most sensitive to reduction of N₂O after the transition to denitrification (Fig. 2, Table 2). Conversely, the greater amounts of N₂O produced by the nutrient rich Sutherland and Asquith soils may have overwhelmed any reduction effect on the SP of N₂O. Our findings attribute ‘N₂O leaky’ soils to excess inorganic N or mineralization potential.

3.3 The ‘hole-in-the-pipe’ influences site preference

As alluded to above, the Bradwell results were most dissimilar to the other soils. It is intriguing that the SP values for the Bradwell soil N₂O never dropped below 14.4‰. While it is clear from the pattern of N₂O fluxes, SP, δ¹⁵N and δ¹⁸O values (Fig. 2) that N₂O production transitioned to denitrification under moist soil conditions (Table 2), it is curious that the SP values were not lower, closer to 0‰, as earlier work demonstrated for denitrification (Denk et al., 2017; Ostrom et al., 2010; Sutka et al., 2006; Toyoda et al., 2005; Winther et al., 2018). Reasons for this discrepancy are as yet unclear, but we are not alone in finding SP values above 0‰ that are attributed to denitrification (Winther et al., 2018). Differences might be related to differences in microbial community structure and activity, though it is also possible that N₂O reduction to N₂ played a larger than anticipated role for the Bradwell soil. Indeed, SP values within the expected range for bacterial denitrification are known to be sensitive to the reduction of N₂O to N₂ (Deppe et al., 2017; Jinuntuya-Nortman et al., 2008; Lewicka-Szczebak et al., 2014; Ostrom et al., 2007; Well and Flessa, 2009).



- Denitrification results in cleavage of the covalent bond between the central N and O in N₂O, and based on kinetic isotope fractionation results in an increase in the ¹⁵N content of the α position of the residual N₂O, thereby increasing the SP (Popp et al., 2002; Ostrom et al., 2007). Thus, the increase in SP in response to N₂O reduction results in a small (but important) shift away from the SP values associated with the origins of denitrification (~ 0‰) towards those of nitrification, i.e., 33‰ (Sutka et al., 2006). Ostrom et al. (2007) showed that the rate of reduction must be substantially greater than 10% of that of production to impact the SP estimates of N₂O from denitrification by more than a few percent. Because it is likely that N₂O consumption was greater than production for the Bradwell soil when soil moisture exceeded 75% WFPS, our results indicate that the ‘size of the hole-in-the-pipe’ may influence denitrification SP to a greater extent than previously documented.
- For N₂O source identification, we adopted an isotopomer mixing approach (Zou et al., 2014; Well et al., 2012) and constructed isotopomer maps (i.e., plots of SP vs. δ¹⁸O) following the procedure of Deppe et al. (2017). This approach allowed us to estimate the impact of N₂O reduction to N₂ on SP. Reduction slopes for our three soils averaged 0.28, which is similar to the average of 0.35 determined by Deppe et al. (2017), but varied over a wide range; i.e., from 0.16 to 0.52 (Fig. 3). A high reduction slope, such as observed for the Bradwell soil, might be associated with the magnitude of N₂O production relative to potential nitrous oxide reductase activity, or conditions that favour more complete stepwise reduction of N₂O to N₂. Whereas the reduction effect on SP might be stronger than previously thought, it may only be observable when conditions are favourable, as evidenced for the Bradwell soil. We echo earlier proposals made by Ostrom et al. (2007), and suggest that the current knowledge and understanding of ¹⁵N₂O isotopomers may have inherent biases due to methodological focus on high flux scenarios – where the rates of N₂O reduction are minor and likely not of sufficient magnitude to alter isotopomer and SP data. Relatively few studies have focused on lower flux scenarios when the rates of N₂O reduction relative to production may exert more of an influence on SP. Our findings support the hypothesis that N₂O reduction is a minor process influencing SP during conditions of high soil N₂O flux, but may be more important for conditions with low N₂O flux (Ostrom et al., 2007).

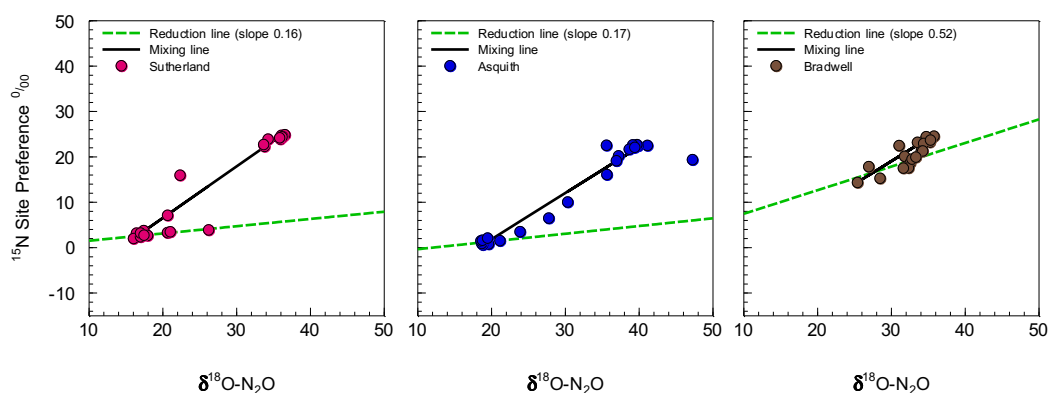


Figure 3 Isotopomer map to determine the source partitioning of N₂O derived from nitrification versus denitrification using ¹⁵N site preference (SP) and δ¹⁸O of N₂O. The linear mixed model approach was based on Deppe et al. 2017, but with end-



members derived from our data (mixing line). The reduction line was placed through the average SP value of gas samples derived from < 60% water-filled pore space range.

5 Due to the wide range of reduction slopes observed in our study – and the differences for how SP is influenced in conditions with high flux vs low flux – we argue that using a single average reduction slope is insufficient to best predict N₂O reduction. It is recommended that further research better quantify the conditions that promote N₂O reduction for improved N₂O source predictions. This could be particularly important for assessing microbial source pathways of N₂O production and consumption across seasonal and spatial scales, because sustained periods of low flux are not uncommon.

10 3.4 Source pathway partitioning and modelling

Using data pooled from the isotopomer maps to model source partitions, linear models were developed that fit the transitions for nitrification-derived N₂O ($R^2 = 0.65, p < 0.001$) and denitrification-derived N₂O ($R^2 = 0.65, p < 0.001$) (Fig. 4) with coefficients of variation and root-mean-square errors of 0.10 and 0.20, respectively. The models predict that over a soil moisture range of 53 to 78% WFPS, the source partitioning rapidly changed from nitrification- to denitrification-dominated N₂O production. At soil moisture levels < 53% WFPS, N₂O was predominately attributed to nitrification ($F_N = 1$) but thereafter decreased rapidly, according to Eq. (6):

$$F_N = 3.19 - 0.041x \quad (6)$$

until a WFPS of 78%. This result was mirrored by the increase in N₂O attributed to denitrification at a WFPS of 53% according to Eq. (7):

$$20 \quad F_D = -2.19 + 0.041x \quad (7)$$

until $F_D = 1$ at 78% and higher WFPS. These relationships exemplify the sensitivity of N₂O production pathways to soil moisture changes. For instance, during the transition, a change in soil moisture as little as 10% (i.e., from 55 to 65% WFPS) is predicted to lower nitrification-derived N₂O production by 56% but increase denitrification-derived N₂O by >7-fold (Fig. 4). Clearly, soil moisture change during the transition is a key regulator of which pathway dominantly produces N₂O—be it nitrification or denitrification, or a mixture of both. Our results largely support earlier studies that evaluated the relationship between soil moisture and N₂O emissions (Davidson, 1991; Linn and Doran, 1984); however, we provide a method that moves beyond just inferring N₂O source pathways towards quantifying the pathway contributions over a range of soil moisture.

30

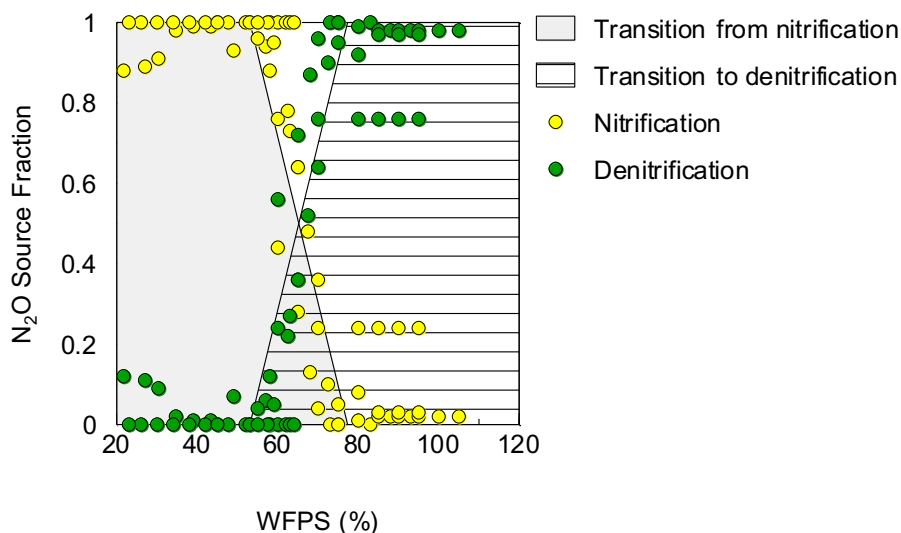


Figure 4 Fraction of emitted N_2O that was attributed to nitrification (yellow points, shaded grey area) or denitrification (green points, lined area) based on the isotopomer mixing model (data points) and as predicted by linear regression (lines).

4 Conclusions

- 5 Determining the production pathways of soil-derived N_2O is a worthwhile goal as there is potential to manage soils in ways that lead to reduced nitrification or denitrification during periods of risk for N_2O loss—thereby mitigating emissions of a potent greenhouse gas. We show that isotopomer data have the potential to provide progress towards this goal. Measuring $^{15}N_2O$ isotopomers enabled a more precise evaluation of the relationship between soil moisture and N_2O production and we present a source fraction model for key soil moisture ranges. In general, our results support
- 10 earlier assumptions about the relationships between moisture and N_2O production pathways but can help move beyond inferring towards quantifying relative source pathways. Clearly, soil moisture level during ‘the transition zone’ is a key regulator of which pathway predominates—be it nitrification, denitrification, or a mixture of both. Hence, the models presented herein should be useful for other researchers to estimate contributions of nitrification versus denitrification when soil WFPS ranges from 53-78%.
- 15 One known caveat when using the isotopomer method for source pathway quantification is the isotope effect of N_2O reduction. Previous researchers have attempted to address this limitation by using an average reduction slope and linear mixed model approach, but due to the wide range of reduction slopes observed in our study—and the differences for how denitrification SP is influenced in conditions with high N_2O flux vs low flux—we argue that using a single average reduction slope is insufficient to best predict N_2O reduction. It is recommended that further research better
- 20 quantify the conditions which influence N_2O reduction and its sensitivity on denitrification SP values for improved N_2O source predictions.



5 Author Contributions

KAC and REF designed the experiment and TP carried it out. KAC prepared the manuscript with contributions from REF and TP.

6 Competing Interests

- 5 The authors declare that they have no conflict of interest.

7 Acknowledgements

- Financial support was provided by the University of Saskatchewan College of Agriculture and Bioresources via a Martin Agricultural Trust Fund award to KAC and REF and by the Natural Sciences and Engineering Research Council of Canada via a Discovery Grant award to KAC. The authors are grateful to Frank Krijnen and Darin Richman
- 10 for technical help in the lab.



8 References

- Balaine, N., Clough, T. J., Beare, M. H., Thomas, S. M., Meenken, E. D. and Ross, J. G.: Changes in Relative Gas Diffusivity Explain Soil Nitrous Oxide Flux Dynamics, *Soil Sci. Soc. Am. J.*, 77(5), 1496–1505, doi:DOI 10.2136/sssaj2013.04.0141, 2013.
- 5 Banerjee, S., Helgason, B., Wang, L., Winsley, T., Ferrari, B. C. and Siciliano, S. D.: Legacy effects of soil moisture on microbial community structure and N₂O emissions, *Soil Biol. Biochem.*, 95, 40–50, doi:10.1016/J.SOILBIO.2015.12.004, 2016.
- Barnard, R., Leadley, P. W. and Hungate, B. A.: Global change, nitrification, and denitrification: A review, *Global Biogeochem. Cycles*, 19(1), doi:10.1029/2004GB002282, 2005.
- 10 Butterbach-Bahl, K., Baggs, E. M., Dannenmann, M., Kiese, R. and Zechmeister-Boltenstern, S.: Nitrous oxide emissions from soils: how well do we understand the processes and their controls?, *Philos. Trans. R. Soc. Lond. B. Biol. Sci.*, 368(1621), 20130122, doi:10.1098/rstb.2013.0122, 2013.
- Chapuis-Lardy, L., Wrage, N., Metay, A., Chotte, J.L. and Bernoux, M.: Soils, a sink for N₂O? A review, *Glob. Chang. Biol.*, 13(1), 1–17, doi:10.1111/j.1365-2486.2006.01280.x, 2007.
- 15 Clough, T. J., Sherlock, R. R. and Rolston, D. E.: A Review of the Movement and Fate of N₂O in the Subsoil, *Nutr. Cycl. Agroecosystems*, 72(1), 3–11, doi:10.1007/s10705-004-7349-z, 2005.
- Davidson, E. A.: Fluxes of nitrous oxide and nitric oxide from terrestrial ecosystems. Pp. 219–235 in Rogers J.E., Whitman, W.B. eds. *Microbial Production and Consumption of Greenhouse Gases: Methane, Nitrogen Oxides and Halomethanes*, Am. Soc. Microbiol. Washington, DC., in *Microbial Production and Consumption of Greenhouse Gases: Methane, Nitrogen Oxides and Halomethanes*, edited by J. E. Rogers and W. B. Whitman, pp. 219–235, Am. Soc. Microbiol., Washington, DC., 1991.
- 20 Denk, T. R. A., Mohn, J., Decock, C., Lewicka-Szczepak, D., Harris, E., Butterbach-Bahl, K., Kiese, R. and Wolf, B.: The nitrogen cycle: A review of isotope effects and isotope modeling approaches, *Soil Biol. Biochem.*, 105, 121–137, doi:10.1016/J.SOILBIO.2016.11.015, 2017.
- 25 Deppe, M., Well, R., Giesemann, A., Spott, O. and Flessa, H.: Soil N₂O fluxes and related processes in laboratory incubations simulating ammonium fertilizer depots, *Soil Biol. Biochem.*, 104, 68–80, doi:10.1016/j.soilbio.2016.10.005, 2017.
- Environment Canada.: *Canadian national Inventory Report: Part 3 Greenhouse gas sources and sinks in Canada*, 2015.
- 30 Van Groenigen, J. W., Huygens, D., Boeckx, P., Kuyper, T. W., Lubbers, I. M., Rütting, T. and Groffman, P. M.: The soil N cycle: new insights and key challenges, *Soil*, 1, 235–256, doi:10.5194/soil-1-235-2015, 2015.
- Jinuntuya-Nortman, M., Sutka, R. L., Ostrom, P. H., Gandhi, H. and Ostrom, N. E.: Isotopologue fractionation during microbial reduction of N₂O within soil mesocosms as a function of water-filled pore space, *Soil Biol.*



- Biochem., 40(9), 2273–2280, doi:10.1016/J.SOILBIO.2008.05.016, 2008.
- Lewicka-Szczebak, D., Well, R., Köster, J. R., Fuß, R., Senbayram, M., Dittert, K. and Flessa, H.: Experimental determinations of isotopic fractionation factors associated with N₂O production and reduction during denitrification in soils, *Geochim. Cosmochim. Acta*, 134, 55–73, doi:10.1016/J.GCA.2014.03.010, 2014.
- 5 Linn, D. M. and Doran, J. W.: Effect of water-filled pore space on carbon dioxide and nitrous oxide production in tilled and nontilled soils, *Soil Sci. Soc. Am. J.*, 48(6), 1267–1272, doi:10.2136/sssaj1984.03615995004800060013x, 1984.
- Maynard, D., Kalra, Y. and Crumbaugh, J.: Nitrate and exchangeable ammonium nitrogen, in *Soil Sampling and Methods of Analysis*, edited by M. R. Carter and E. G. Gregorich, pp. 71–80, CRC Press, Boca Raton, Florida,
- 10 2007.
- Mohn, J., Wolf, B., Toyoda, S., Lin, C. T., Liang, M. C., Brüggemann, N., Wissel, H., Steiker, A. E., Dyckmans, J., Szwec, L., Ostrom, N. E., Casciotti, K. L., Forbes, M., Giesemann, A., Well, R., Doucett, R. R., Yarnes, C. T., Ridley, A. R., Kaiser, J. and Yoshida, N.: Interlaboratory assessment of nitrous oxide isotopomer analysis by isotope ratio mass spectrometry and laser spectroscopy: current status and perspectives, *Rapid Commun. Mass Spectrom.*,
- 15 28(18), 1995–2007, doi:10.1002/rcm.6982, 2014.
- Ostrom, N. E., Pitt, A., Sutka, R., Ostrom, P. H., Grandy, A. S., Huizinga, K. M. and Robertson, G. P.: Isotopologue effects during N₂O reduction in soils and in pure cultures of denitrifiers, *J. Geophys. Res.*, 112, G02005, doi:10.1029/2006JG000287, 2007.
- Ostrom, N. E., Sutka, R., Ostrom, P. H., Grandy, A. S., Huizinga, K. M., Gandhi, H., von Fischer, J. C. and
- 20 Robertson, G. P.: Isotopologue data reveal bacterial denitrification as the primary source of N₂O during a high flux event following cultivation of a native temperate grassland, *Soil Biol. Biochem.*, 42(3), 499–506, doi:10.1016/J.SOILBIO.2009.12.003, 2010.
- Popp, B. N., Westley, M. B., Toyoda, S., Miwa, T., Dore, J. E., Yoshida, N., Rust, T. M., Sansone, F. J., Russ, M. E., Ostrom, N. E. and Ostrom, P. H.: Nitrogen and oxygen isotopomeric constraints on the origins and sea-to-air flux
- 25 of N₂O in the oligotrophic subtropical North Pacific gyre, *Global Biogeochem. Cycles*, 16(4), 12-1-12–10, doi:10.1029/2001GB001806, 2002.
- Reynolds, W. D. and Topp, G. C.: Soil Water Desorption and Imbibition: Long Column, in *Soil Sampling and Methods of Analysis*, edited by M. R. Carter and E. G. Gregorich, pp. 999–1006., 2007.
- Sutka, R. L., Ostrom, N. E., Ostrom, P. H., Breznak, J. A., Gandhi, H., Pitt, A. J. and Li, F.: Distinguishing nitrous
- 30 oxide production from nitrification and denitrification on the basis of isotopomer abundances., *Appl. Environ. Microbiol.*, 72(1), 638–44, doi:10.1128/AEM.72.1.638-644.2006, 2006.
- Toyoda, S., Mutoke, H., Yamagishi, H., Yoshida, N. and Tanji, Y.: Fractionation of N₂O isotopomers during production by denitrifier, *Soil Biol. Biochem.*, 37(8), 1535–1545, doi:10.1016/j.soilbio.2005.01.009, 2005.
- Wagner-Riddle, C., Congreves, K. A., Abalos, D., Berg, A. A., Brown, S. E., Ambadan, J. T., Gao, X. and Tenuta,



- M.: Globally important nitrous oxide emissions from croplands induced by freeze-thaw cycles, *Nat. Geosci.*, 10(4), doi:10.1038/ngeo2907, 2017.
- Well, R. and Flessa, H.: Isotopologue signatures of N₂O produced by denitrification in soils, *J. Geophys. Res. Biogeosciences*, 114, doi:10.1029/2008JG000804, 2009.
- 5 Winther, M., Balslev-Harder, D., Christensen, S., Priemé, A., Elberling, B., Crosson, E. and Blunier, T.: Continuous measurements of nitrous oxide isotopomers during incubation experiments, *Biogeosciences*, 15, 767–780, doi:10.5194/bg-15-767-2018, 2018.

**Table 1 Soil physical and chemical characteristics.**

	Sutherland	Asquith	Bradwell
Previous cropping history	Vegetable crops	Fodder crops	Field crops
Texture class	Silty clay loam	Sandy loam	Loam
Organic matter (%)	5.9	3.9	2.7
Equilibrium soil water (θ_g)	0.46	0.40	0.33
pH	7.6	7.5	7.9
CEC $\text{cmol}_c \text{kg}^{-1}$	34.8	18.6	16.9
Total N (%)	0.42	0.21	0.16
Total ^{15}N (atom %)	0.371	0.370	0.368
Nitrate ($\mu\text{g g}^{-1}$)	194	35	10
Ammonium ($\mu\text{g g}^{-1}$)	3.8	1.7	5.2
Bray-Phosphorus (ppm)	542	190	23
Potassium (ppm)	1415	544	329
Sulfur (ppm)	49	28	13
Magnesium (ppm)	925	448	432
Calcium (ppm)	4650	2670	2490



Table 2. Linear regressions between ^{15}N site preference and soil water-filled pore space (%) during three soil moisture regions for each soil type: i) before the transition from nitrification, ii) during the transition from nitrification to denitrification, and iii) after the transition to denitrification.

Soil type	WFPS (%)	Slope	Intercept	Pearson r	<i>p</i> -value
Before transition					
Sutherland	< 64	-0.049	26.69	-0.30	0.4660 ^{ns}
Asquith	< 58	-0.004	22.04	-0.04	0.8973 ^{ns}
Bradwell	< 63	0.010	22.69	0.14	0.6781 ^{ns}
During transition					
Sutherland	64 – 83	-0.99	81.62	0.88	0.0214*
Asquith	58 – 73	-1.19	85.75	-0.89	0.0067**
Bradwell	63 – 75	-0.59	58.29	-0.99	0.0004*
After transition					
Sutherland	> 83	0.065	-3.01	0.86	0.0126*
Asquith	> 73	0.072	-4.77	0.99	0.0064**
Bradwell	> 75	0.262	-4.47	0.94	0.0154*

5